NATIONAL AERONAUTICS AND SPACE ADMINISTRATION

Technical Report 32-1367

Analysis of Space Vehicle Structures Using the Transfer-Function Concept

E. Heer

M. R. Trubert

JET PROPULSION LABORATORY

CALIFORNIA INSTITUTE OF TECHNOLOGY

PASADENA, CALIFORNIA

April 1, 1969

NATIONAL AERONAUTICS AND SPACE ADMINISTRATION

Technical Report 32-1367

Analysis of Space Vehicle Structures Using the Transfer-Function Concept

E. Heer
M. R. Trubert

JET PROPULSION LABORATORY
CALIFORNIA INSTITUTE OF TECHNOLOGY
PASADENA, CALIFORNIA

April 1, 1969

TECHNICAL REPORT 32-1367

Prepared Under Contract No. NAS 7-100
National Aeronautics and Space Administration

Preface

The work described in this report was performed by the Engineering Mechanics Division of the Jet Propulsion Laboratory.

Contents

Figures

Contents (contd)

Figures (contd)

Abstract

In this report the concept of frequency transfer function is used for the analysis of space vehicle structures. The method of determining the dynamic response of a structural system from the subsystems' characteristics is given a review and is explored for applications to space vehicle systems. The basic problem is considered to be that of joining together and determining the dynamic response of a number of subsystems that may be excited by deterministic and/or stationary random multiple inputs. The subsystems may represent, for instance, a launch vehicle, a spacecraft, an entry capsule, and a lander system; or they may represent a structure under test and a system of shakers that substantially influence the experimental results during dynamic testing, the effects of which are to be eliminated so that the true transfer functions can be obtained. The specific objectives of this paper are to present a unifying and general picture of the transfer-function technique and to illustrate with a number of examples its practical utility in actual life situations as they have been encountered at the Jet Propulsion Laboratory (JPL).

Analysis of Space Vehicle Structures Using the Transfer-Function Concept

I. Introduction

During recent years, analysts have directed their attention to the design, analysis, and evaluation of the general dynamical and vibrational behavior of space vehicle systems with ever-increasing complexity. In these endeavors, the characterization of the dynamic properties of linear systems by the frequency-dependent ratios between inputs and outputs, i.e., transfer functions, has become a well-established concept and its application has proved of great value, particularly in connection with work related to subsystem coupling techniques in which experimental and flight measurement data have to be utilized.

While it is desirable to consider the complete system at once, a direct dynamic analysis of large space vehicle systems may not be practicable, even with the most powerful computer presently available. Similarly, it is frequently not feasible to conduct dynamic tests of complete space vehicle systems because of their size, or because different parts of these systems are fabricated and assembled at different geographical locations. A method of first dividing the system into suitable subsystems and then determining the system response from the subsystem characteristics, such as transfer functions, therefore has definite advantages, particularly when some subsystems already have flight qualification and are to be combined with different new subsystems, as e.g., in the *Apollo*, *Surveyor*, and *Mariner* space programs.

This then requires a method by which knowledge of the computed or measured transfer functions of the component parts of the system allows the prediction of the vibrational response of the whole system (Refs. 1, 2). Methods of analyzing dynamic systems based on subsystem characteristics have been advocated in one form or another by a number of authors (Refs. 3–9), and a digital computer program has been developed (Ref. 10) and successfully applied (Ref. 11). For a purely analytical analysis using a modal approach, the developments by Hurty (Ref. 6) and Bamford (Ref. 10) are in most cases suitable for the analysis of the coupled system. However, if subsystem characteristics are determined experimentally, it is convenient to use the concept of transfer function for the response analysis of the coupled system.

In this paper the definition of transfer function is taken in its broadest sense as: the steady-state response at one point due to a unit amplitude sinusoidal input at another point. Thus, the various concepts of mobility, impedance, receptance, and the like are included in this definition but, once a particular choice has been made, consistency is required, of course.

II. Theory of Subsystem Coupling

A. System Representation

A system is considered composed of N arbitrarily interconnected subsystems, illustrated in Fig. 1. The impressed excitations are the Fourier transforms of their respective time histories $\{p(t)\}$, i.e., the excitation vector $\{P(\omega)\}$ of the entire system in the frequency domain, given by

$$\{P(\omega)\} = \int_{-\infty}^{\infty} \{p(t)\}\, e^{-i\omega t}\, dt \qquad (1)$$

Similar remarks apply to the frequency response vector $\{X(\omega)\}$, from which the corresponding time response vector $\{x(t)\}$ is obtained by the Fourier inversion

$$\{x(t)\} = \frac{1}{2\pi} \int_{-\infty}^{\infty} \{X(\omega)\}\, e^{i\omega t}\, d\omega \qquad (2)$$

Hence, all quantities introduced in Fig. 1 are, in general, steady-state complex numbers at frequency ω.

For practical reasons, because in most cases deformable rather than rigid connections are required between the subsystem's coupling points, it is assumed that the interconnections consist of discrete, massless coupling units (Ref. 1). These coupling units are characterized by their assumed or measured compliances $K_{m_c}(\omega)$, which are, in general, frequency-dependent, complex functions.

In Fig. 1, boundary conditions are not explicitly indicated, but are implied. For instance, a space vehicle in flight has no external restraints, and the system can be represented as shown in Fig. 1. However, a similar representation can also be used when, for instance, prelaunch conditions are considered, where the space vehicle is on the launch pad, and at least one of the subsystems is restrained to the launch pad. In this case, the launch pad becomes one of the subsystems appropriately interconnected with the space vehicle subsystems.

Another case of considerable importance exists when one of the subsystems is a linear feedback control system. In this case the appropriate outputs are fed back as inputs in Fig. 1 to form the required control loops.

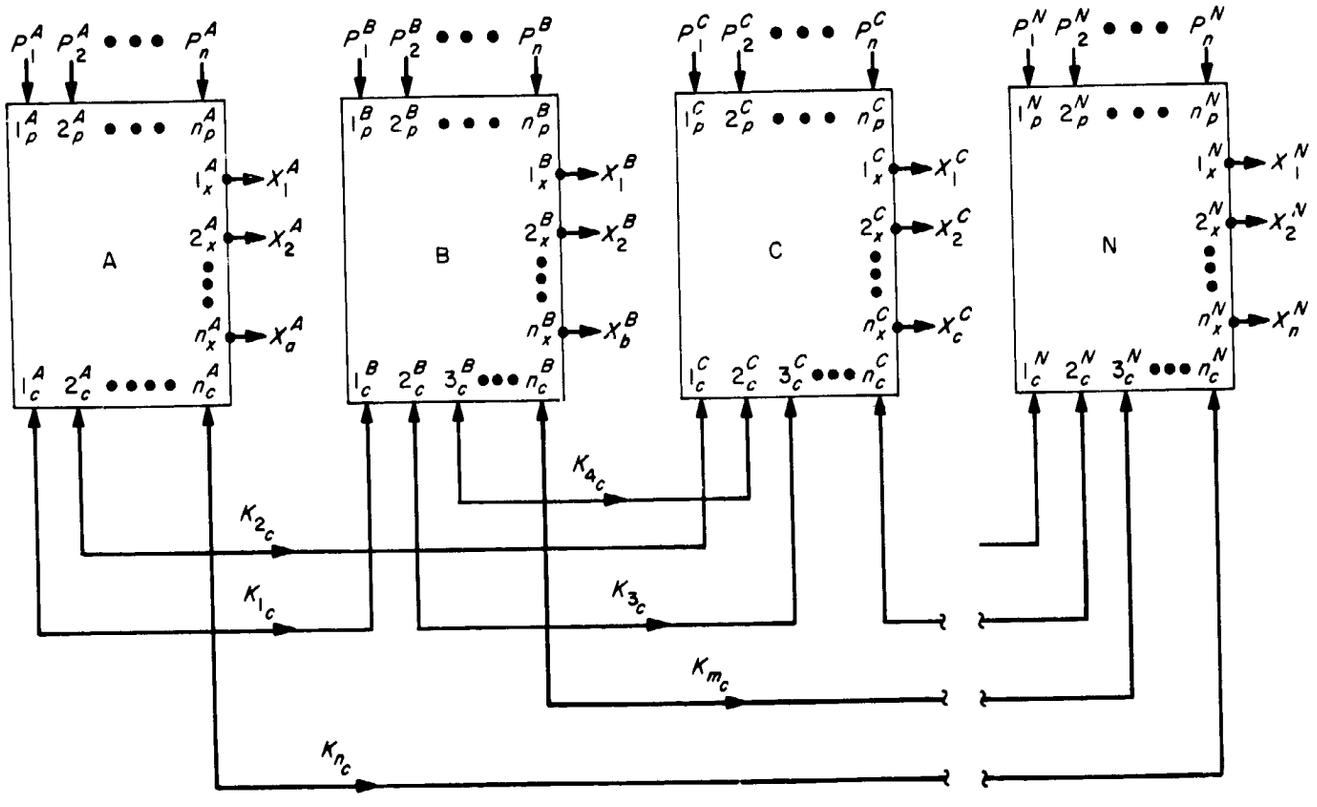

Fig. 1. Representation of system consisting of N coupled systems

B. Component Transfer Functions

The component transfer functions $\theta^J_{ij}(\omega)$ between the typical points i and j in subsystem J can be determined analytically or experimentally. Because of the ever-present damping, there exists a phase lag between the amplitudes of excitation and response. The transfer functions, therefore, appear in general as complex numbers, where both the real and imaginary part, or equivalently, the modulus and phase angle are given as functions of frequency ω.

Analytically, a modal analysis gives the normal modes V_{ik} representing the response of the k^{th} mode at point i, the modal frequencies ω_k, and the generalized masses m_k. For example, the displacement transfer function or receptance is then, assuming small or proportional damping,

$$\theta^J_{ij}(\omega) = \sum_k \frac{V_{ik} V_{jk}}{m_k \left[(\omega_k^2 - \omega^2) + i2\beta_k \omega_k \omega \right]} \qquad (3)$$

where β_k is an assumed or measured (in general, frequency-dependent) damping factor. For the rigid body modes, i.e., rigid translation and rotation, the corresponding eigenfrequencies in Eq. (3) are zero. Other types of transfer functions can be derived from Eq. (3). For instance, velocity and acceleration transfer functions are obtained by multiplying through by $(i\omega)$ and $(-\omega^2)$, respectively.

Experimentally, as diagrammed in Fig. 2, the transfer functions are determined by exciting the structure with a shaker producing an input force that closely approximates a sine wave, the frequency of which is slowly varied (sine sweep), and monitoring the output response. After proper filtering through an analog processing system to extract the fundamental components of the signals, the modulus of the output/input ratio and the phase angle between input and output are recorded in terms of the frequency and subsequently digitized.

In analytical determinations of component transfer functions, the appropriate boundary conditions are imposed during the modal analysis as required by the assumed model. However, in experimental work it is often expedient and applicable with general validity to determine the transfer functions for the free, unrestrained subsystems. This can be accomplished through several techniques. For instance, the "soft spring" technique, where the rigid body soft-spring frequencies are far below the fundamental distortion frequency, is often applicable. On the other hand, it is often possible to take

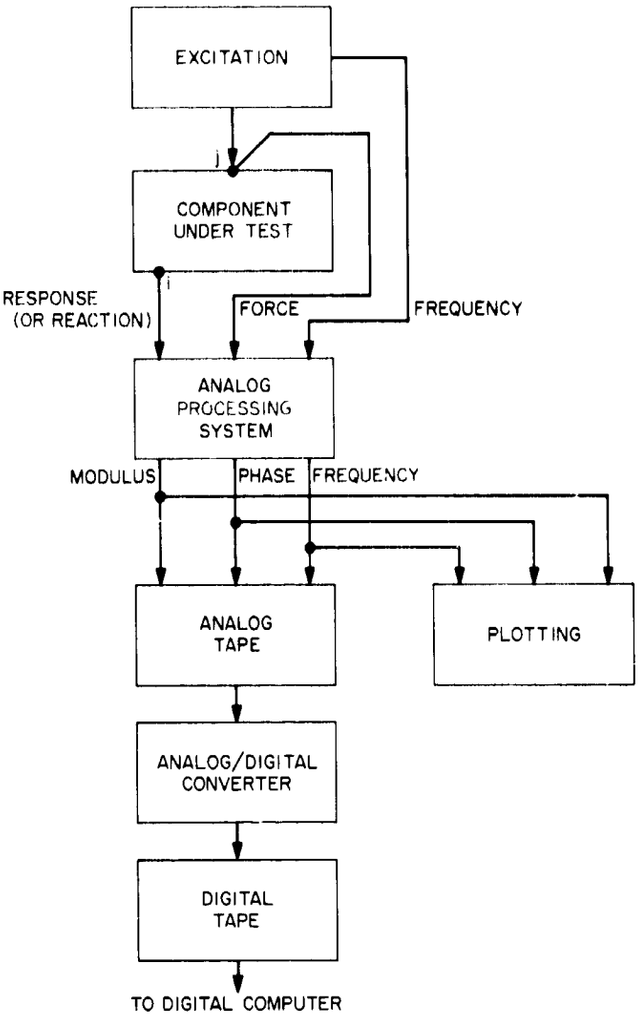

Fig. 2. Experimental determination of transfer functions

advantage of the subsystem's symmetry axes or symmetry planes, where the supports can be arranged so that they have no influence on the response of interest during the test. A more general approach is to support the subsystem during the test elastically at the test points and simultaneously measure, for each support excitation at a point, all the support forces and support displacements, as illustrated in Fig. 3. As discussed below, the effects of this experimental equipment can then be extracted by digital means, thus giving the transfer functions of the unrestrained system.

C. The System Matrix

After the analytically and/or experimentally determined component transfer functions are available, it is the objective to express the response vector $\{X(\omega)\}$ of the

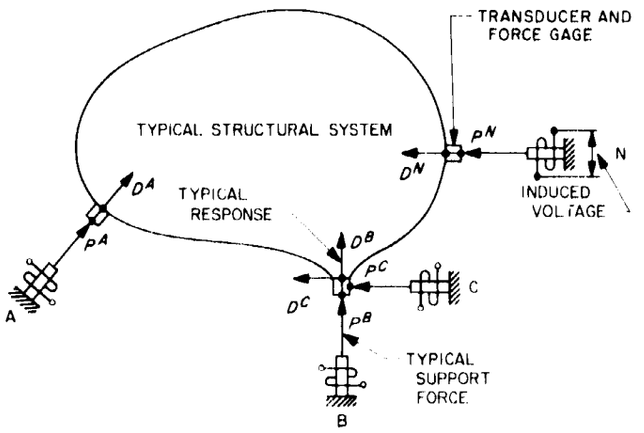

Fig. 3. Multiple shaker excitation of structural system with simultaneous measurement of all support forces and responses for induced excitation at one or several supports

coupled system in terms of the excitation vector $\{P(\omega)\}$ as follows:

$$\{X(\omega)\} = [H(\omega)]\,\{P(\omega)\} \tag{4}$$

The system matrix of transfer functions, $[H(\omega)]$, is obtained from (Refs. 1, 2)

$$[H] = \left[[\bar{\mathcal{D}}] + [{}^{*}\bar{\mathcal{D}}]\,[\overset{T}{C}]\,[A]\,[C]\,[\bar{\bar{\mathcal{D}}}] \right] \tag{5}$$

where

$$[A] = \left[\lceil K \rfloor - [C]\,[\bar{\bar{\bar{\mathcal{D}}}}]\,[\overset{T}{C}] \right]^{-1} \tag{6}$$

In Eqs. (5) and (6), $[\mathcal{D}]$, $[{}^{*}\bar{\mathcal{D}}]$, $[\bar{\bar{\mathcal{D}}}]$, and $[\bar{\bar{\bar{\mathcal{D}}}}]$ are matrices of the subsystem transfer functions, involving, respectively, response and excitation points, response and coupling points, only coupling points, and coupling and excitation points. The coupling (compatibility) matrix $[C]$ is a real rectangular matrix having only two nonzero elements in each row, (-1) and $(+1)$, and $\lceil K \rfloor$ is the diagonal constrained matrix, which includes the coupling units K_{m_r}.

D. Deterministic and Random Excitations

If the excitation time histories in the vector $\{p(t)\}$ are deterministic, the responses will also be deterministic, and each element of the frequency response vector $\{X(\omega)\}$ can be transformed into the corresponding time history using Eq. (2), thus giving the time response vector $\{x(t)\}$ for the coupled system. On the other hand, if the system is subjected to stationary random excitations, the excitation cross-correlation functions $R_{\ell m}^{LM}(\tau)$ and the excitation cross-power spectral densities $S_{\ell m}^{LM}(\omega)$ between point ℓ in subsystem L and point m in subsystem M are obtained (Ref. 1) in the following form, respectively:

$$R_{\ell m}^{LM}(\tau) = \lim_{T\to\infty} \frac{1}{T} \int_{-T/2}^{T/2} p_{\ell}^{L}(t)\, p_{m}^{M}(t+\tau)\, dt \tag{7}$$

and

$$S_{\ell m}^{LM}(\omega) = \int_{-\infty}^{\infty} R_{\ell m}^{LM}(\tau)\, e^{-i\omega\tau}\, d\tau \tag{8}$$

The response cross-power spectral densities ${}^{*}S_{jk}^{JK}(\omega)$ between point j in subsystem J and point k in subsystem K are then obtained from Eqs. (5) and (8) as

$${}^{*}S_{jk}^{JK}(\omega) = \sum_{\ell=1}^{\ell_p} \sum_{m=1}^{m_p} \sum_{L=A}^{N} \sum_{M=A}^{N} {}^{*}H_{j\ell}^{JL}(\omega)\, H_{km}^{KM}(\omega)\, S_{\ell m}^{LM}(\omega) \tag{9}$$

In Eq. (9), the right-hand terms are: the complex conjugate of the system transfer function between point j in component system J and point ℓ in component system L; the system transfer function between point k in component system K and point m in component system M; the excitation cross-power spectral density between point ℓ in component system L and point m in component system M. It is clear that the response-power spectral density at point j in component system J is obtained from Eq. (9) by setting $K = J$ and $k = j$.

III. Problems of Implementation

A. Receptance Coupling Program

The receptance coupling program (RECEP) (Ref. 12) was based originally on the concept of receptances; however, it can also be applied using general transfer functions as long as consistency is preserved. The program is divided into four basic operations, as shown in the flow diagram in Fig. 4: (1) computation of the matrix $[A]$ of Eq. (6); (2) computation of the system matrix $[H]$

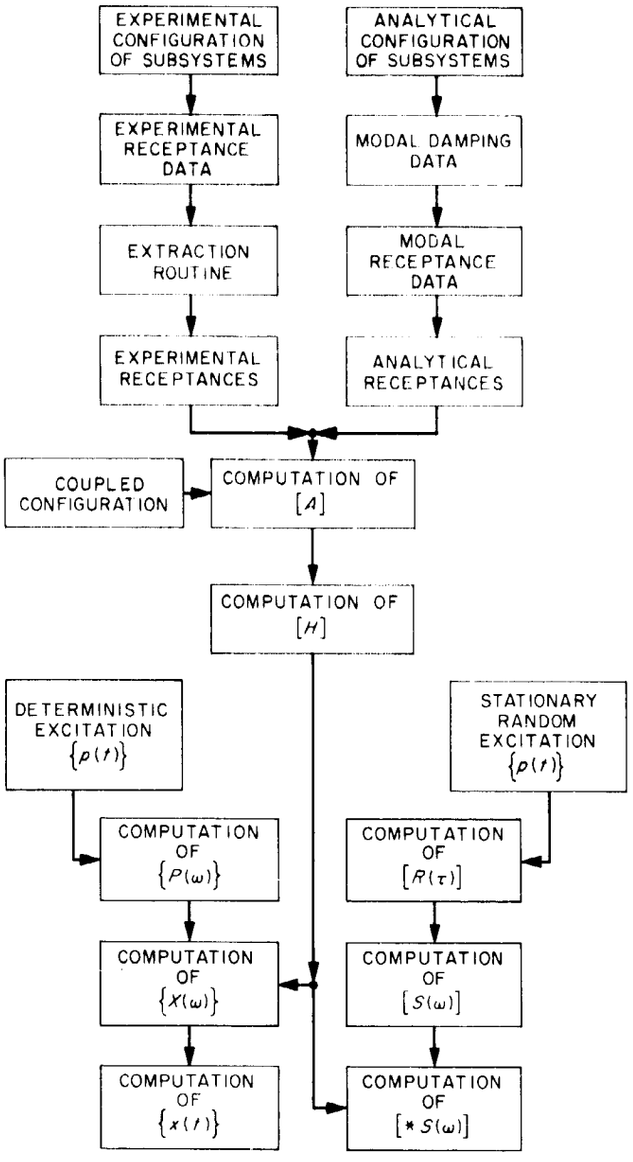

Fig. 4. Functional flow diagram of the receptance coupling program

of Eq. (5); (3) computation of the deterministic time response $\{x(t)\}$; or (4) computation of the spectral densities [*S] due to random excitations.

In the present design of RECEP, up to 70 coupling joints can be handled. The maximum number of excitation points in the entire system may be up to 120 and may be distributed unevenly among the subsystems so that no subsystem has more than 80 excitation points. A similar statement holds for the response points. Because of the large amount of input data that has to be usually handled, an automatic transfer of the subsystem transfer-function data is provided for in RECEP.

B. Component Resonance

In practice, computational difficulties may arise at a number of frequencies that are resonance frequencies for one or more of the uncoupled subsystems. Close to or at these frequencies, certain transfer functions, e.g., receptances and mobilities, of the respective subsystems become very large as compared to those of subsystems not at resonance. Since in general the subsystem resonance frequencies do not coincide with those of the coupled system, the transfer functions of the former will also be large compared to the latter. Thus, it is often necessary to compute "normal size" transfer functions (reflecting no resonance) by taking differences between very large terms that reflect subsystem resonance. Near such resonance frequencies of some subsystems, the transfer-function terms in Eq. (5) will be large. To improve the accuracy of the computation, let $0(\lambda)$, where $0(\lambda) >> 1$, stand for these terms, and $0(1)$ for the nonresonance transfer functions; it is then shown (Ref. 13) that the $0(\lambda)$ parts of each matrix in Eq. (5) are parallel in the sense of parallel vectors in multidimensional space. By a new formulation of the problem, the large parallel parts are removed from the matrices of Eq. (5), which gives an entirely equivalent transfer-function matrix formulation with greatly improved computational accuracy near a subsystem resonance. This improvement is incorporated in the RECEP program.

C. Effects of Measurement Instrumentation

When the transfer functions of a structural system are measured, there are necessarily moving parts such as transducers, force gages, etc., attached at the test points (Fig. 3). If the number of moving parts and/or their mass is large enough, the measured results are often considerably distorted from their true values. It has been shown (Ref. 2) that with the application of the transfer-function coupling technique, the corrected transfer functions can be computed from the measured transfer functions, from the measured supporting forces as mentioned in Section II-B, and from knowledge of the equipment transfer functions. The matrix of the corrected transfer functions is given by the following expression: (Ref. 2)

$$[\theta] = [D]\left[\left[\left[\bar{\bar{\alpha}} - K\right]^{-1}\left[\left[\bar{\alpha}\right][P] - [D]\right]\right]\right]^{-1} \quad (10)$$

where the measured displacements and forces are, respectively,

$$|D| = \begin{bmatrix} D^{1,1} & \cdots & D^{1,N} \\ \vdots & & \vdots \\ D^{N,1} & \cdots & D^{N,N} \end{bmatrix}, \quad |P| = \begin{bmatrix} P^{1,1} & \cdots & P^{1,N} \\ \vdots & & \vdots \\ P^{N,1} & \cdots & P^{N,N} \end{bmatrix} \tag{11}$$

The second superscript, e.g., N, indicates that the data were obtained while shaker N was excited. By exciting all shakers, one at a time, the columns of the matrices in Eq. (11) are determined. In Eq. (10) the $\bar{\bar{\alpha}}$ are the known coupling-point transfer functions of the shakers and the $\bar{\alpha}$ are the known cross-transfer functions between the coupling and force points of the shakers. The K are coupling units (compliances) that play the same role as those discussed in Section II-A. Equation (10) is incorporated as a subroutine in the RECEP program (Fig. 4).

A simple example (Ref. 2) for the application of Eq. (10) is a free-free beam with two shaker mountings as shown in Fig. 5. The measured and the corrected acceleration-transfer-function amplitudes between points 1 and 2 in Fig. 5 are presented for comparison in Figs. 6 and 7. For linear systems the corrected θ_{12} and θ_{21} should be equal. A comparison of these two independently measured and computed transfer functions is given in Fig. 8. While the frequencies of the peak responses agree quite well, there are unfortunately many discrepancies in the amplitudes and frequencies at the point of antiresonance between 25 and 35 Hz. These are attributed partially to the simplifying assumptions for the calculations and partially to insufficiently developed measurement techniques.

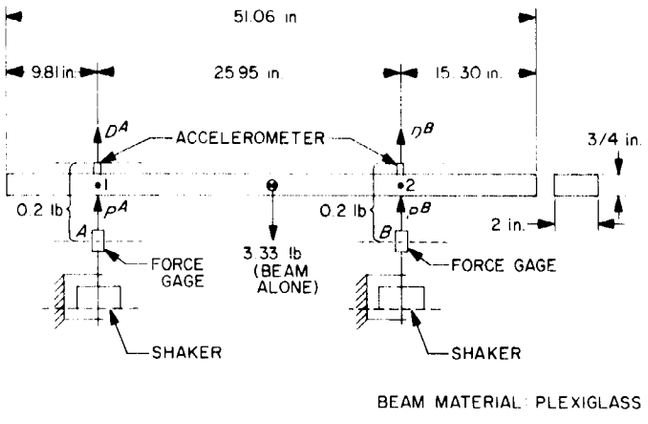

Fig. 5. Free-free beam and shaker configuration for transfer function measurement

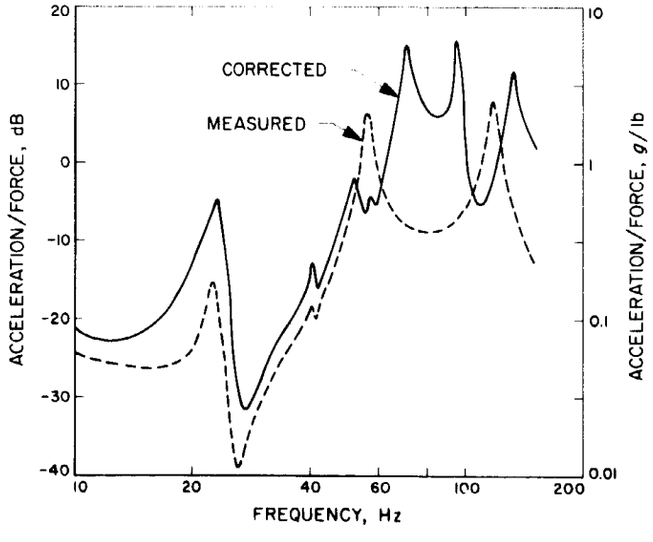

Fig. 6. Comparison of measured and corrected transfer function θ_{12}

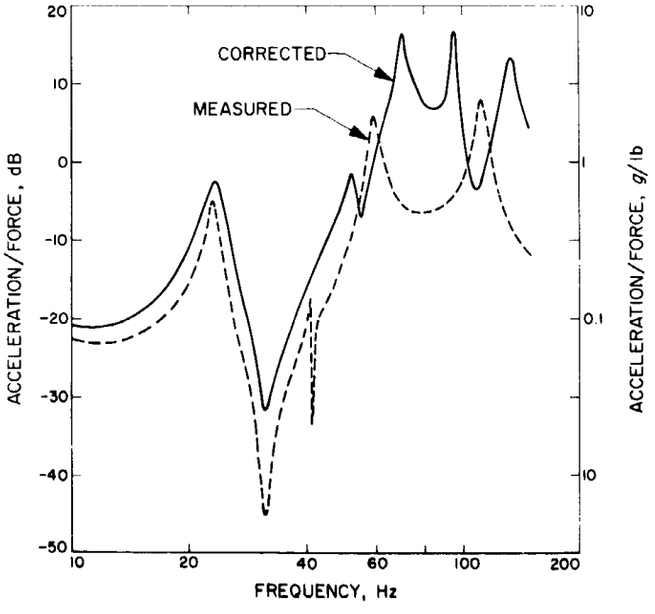

Fig. 7. Comparison of measured and corrected transfer function θ_{21}

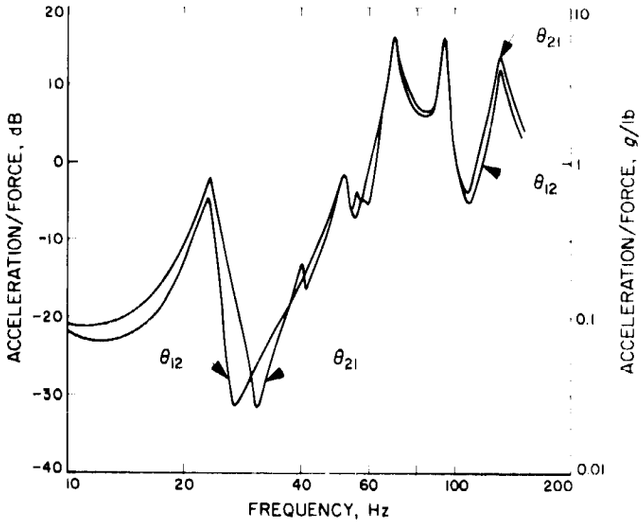

Fig. 8. Comparison of the corrected (computed) transfer functions θ_{12} and θ_{21}

IV. Practical Applications

A. *Surveyor, Mariner,* and *Orbiting Geophysical Observatory (OGO)* Response Prediction From *Ranger* Flight Data

The frequency transfer function approach for structural problems has also been used at JPL for load prediction of certain types. For example, this approach was used to predict the torsional load for the *Surveyor*, *Mariner 67*, and *OGO* spacecraft at booster engine cutoff, making use of the flight data obtained during the Ranger spacecraft series. After close investigation, the frequency domain approach appeared to be the only satisfactory solution to the problem (Refs. 14, 15).

In the examples shown in Fig. 9, the problem was the following. A strong torsional acceleration $\ddot{x}_j^{(1)}(t)$ of a transient nature was observed at the base of the spacecraft during the boosted flight of the *Ranger* series, and it was postulated with a reasonable degree of confidence that this torsional acceleration was due to a spurious transient torque $p_i(t)$ developed by the *Atlas* engine at booster engine cutoff event (BECO). Since the *Surveyor*, *Mariner*, and *OGO* spacecraft used the same *Atlas* booster, it was anticipated that these spacecraft would be subjected to the same type of disturbance at BECO. However, since the upper structures, second stage and spacecraft, were different, the base acceleration $\ddot{x}_j^{(2)}(t)$ was expected to be different from $\ddot{x}_j^{(1)}(t)$. Therefore, the torque $p_i(t)$ at the *Atlas* engine had to be determined. This is an unusual situation which can be called an inverse problem, where the response $\ddot{x}_j^{(1)}(t)$ of a structure (*Atlas/Agena/Ranger*) is known and the forcing function $p_i(t)$ that causes this response is the unknown. Further, because the response and the forcing function are at different locations j and i, it can be shown (Ref. 15) that the time domain approach to this problem can lead to an unstable system of equations. This instability was actually found for the example *Atlas/Agena/Ranger* vehicle. On the other hand, the frequency domain approach avoids this instability since the homogeneous solutions of the equations are removed, dealing exclusively with the complementary solution (Ref. 15).

Calling $X_j^{(1)}(\omega)$ and $P_i(\omega)$ the Fourier transforms of $\ddot{x}_j^{(1)}(t)$ and $p_i(t)$, and $\theta_{ij}^{(1)}(\omega)$ the transfer function between the *Atlas* engine and the base of the spacecraft (Ref. 15), one has according to Eq. (4),

$$X_j^{(1)}(\omega) = \theta_{ij}^{(1)}(\omega)\, P_i(\omega) \tag{12}$$

where the transfer function,

$$\theta_{ij}^{(1)}(\omega) = \sum_k \frac{V_{ik}^{(1)}\, V_{jk}^{(1)}}{m_k \left[1 - \left(\frac{\omega_k}{\omega} \right)^2 - i2\,\beta_k \frac{\omega_k}{\omega} \right]} \tag{13}$$

differs from Eq. (3) by a factor of $-\omega^2$ to shift from the force displacement transfer function to the force acceleration transfer function.

Equation (12) is then rewritten, since contrary to the classical problem the response $X_j^{(1)}(\omega)$ is known and the forcing function $P_i(\omega)$ is the unknown:

$$P_i(\omega) = \frac{X_j^{(1)}(\omega)}{\theta_{ij}^{(1)}(\omega)} \tag{14}$$

Therefore, from a sys em view point one has the situation shown in Fig. 10. Turning now to the new structure, e.g., the *Atlas/Centaur/Surveyor*, one has similarly,

$$X_j^{(2)}(\omega) = \theta_{ij}^{(2)}(\omega)\, P_i(\omega) \tag{15}$$

where the superscript (2) indicates that all parameters are for the new structure (Fig. 11).

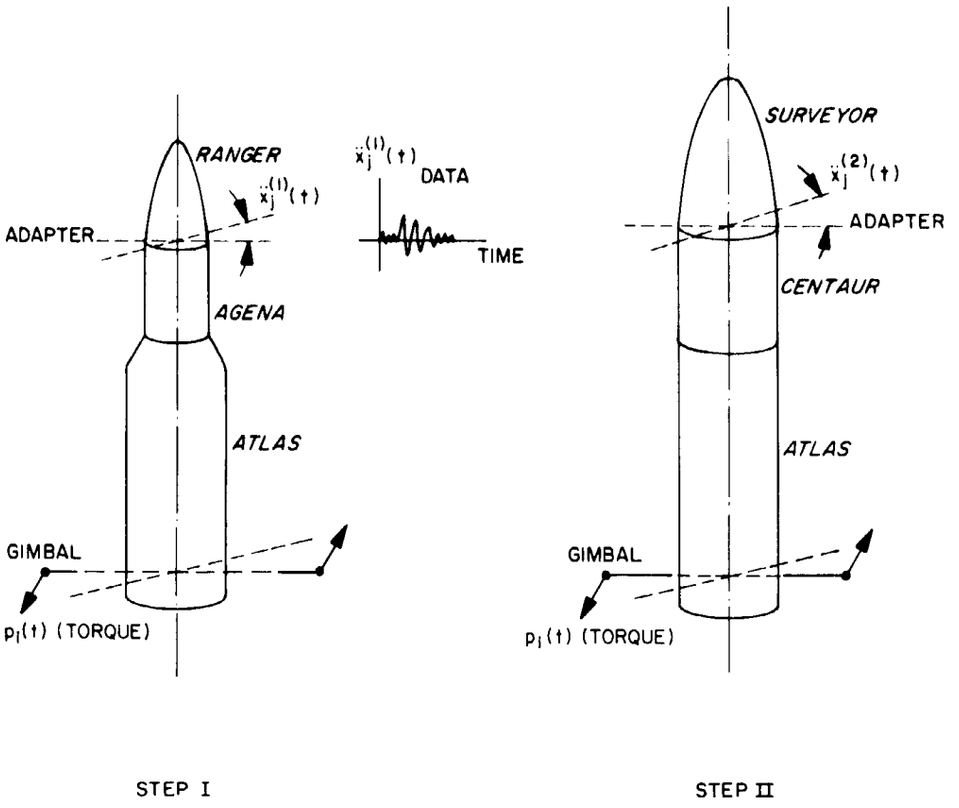

Fig. 9. *Surveyor* torsional load analysis and torsional test

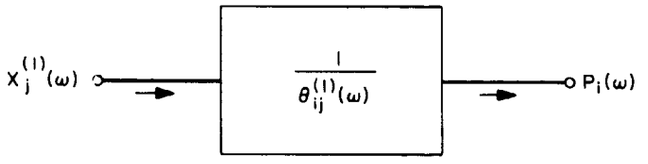

Fig. 10. Input-output diagram for *Atlas/Agena/Ranger* vehicle

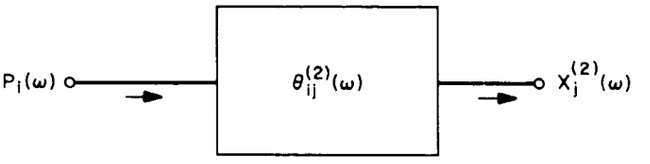

Fig. 11. Input-output diagram for *Atlas/Centaur/Surveyor* vehicle

Finally, one can completely eliminate the unknown torque $P_i(\omega)$ and write

$$X_j^{(2)}(\omega) = \frac{\theta_{ij}^{(2)}(\omega)}{\theta_{ij}^{(1)}(\omega)} X_j^{(1)}(\omega) \qquad (16)$$

The time history of the acceleration $\ddot{x}^{(2)}(t)$ of the new vehicle is obtained by inverse Fourier transform as shown by Eq. (2).

A digital computer program, which numerically computes Fourier transform, inverse Fourier transform, and transfer function for this particular type of problem, has been written (Ref. 15) and used for the *Surveyor*, *Mariner*, and *OGO* spacecraft. Figures 12 through 17 show the actual time histories and Fourier transforms of the responses $\ddot{x}_i^{(1)}(t)$ and $\ddot{x}_i^{(2)}(t)$ for the *Surveyor* spacecraft. Note that $f = \omega/2\pi$ in these figures.

B. Multiple Shaker Environment Simulation

Another problem in which the frequency domain point of view has been found useful at JPL is that of equalization in the multiple shaker excitation for environmental

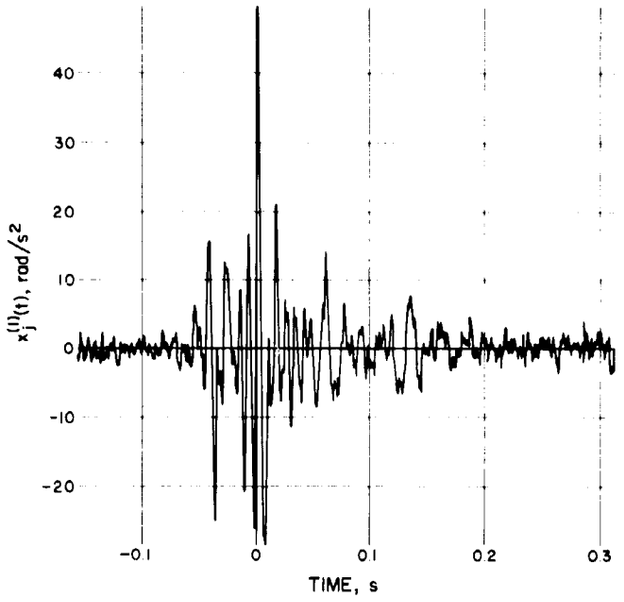

Fig. 12. Input torsional acceleration; *Ranger VIII* data

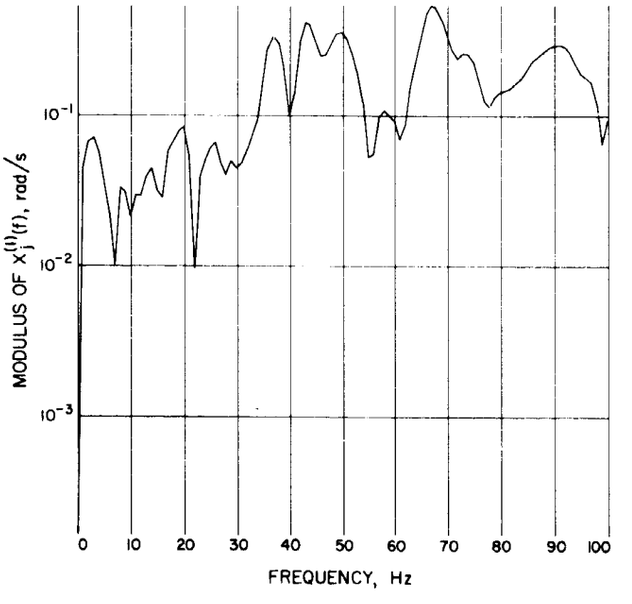

Fig. 13. Fourier transform of input acceleration; modulus

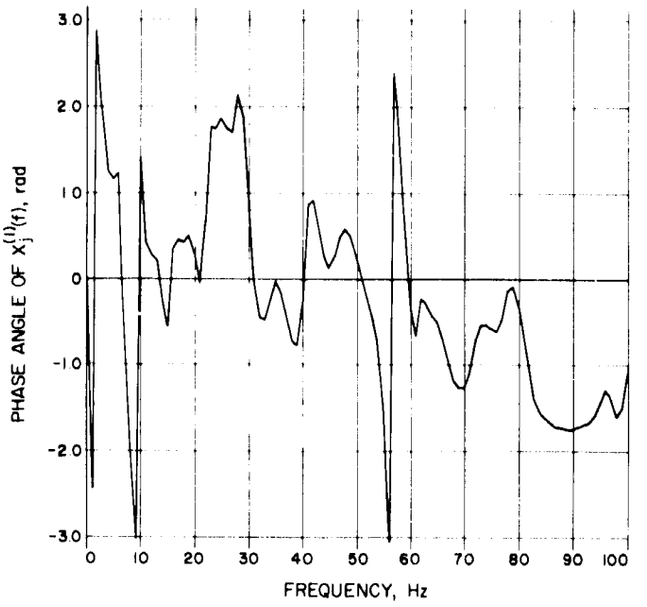

Fig. 14. Fourier transform of input acceleration; phase angle

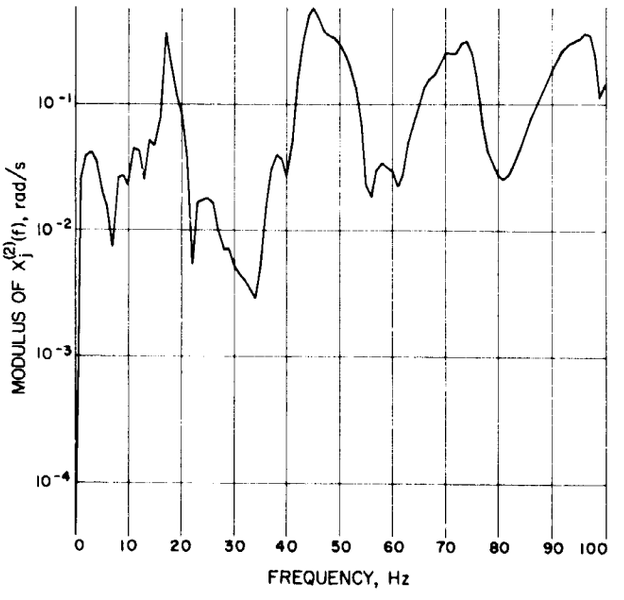

Fig. 15. Fourier transform of *Surveyor* field joint acceleration; modulus

testing. In this problem the structure (Fig. 3) is to be excited at n locations by N shakers ($N \leq 3n$) in order to reproduce given accelerations (Refs. 16, 17) $a_1(t)$, $a_2(t)$, $\cdots$, $a_N(t)$ at those locations. Electrodynamic shakers driven by electronic power amplifiers are currently used for this type of test to apply the necessary forces. The unknowns of the problem are the shaker voltages $e_1(t)$, $e_2(t)$, $\cdots$, $e_N(t)$ that are obtained from the accelerations $a_1(t)$, $a_2(t)$, $\cdots$, $a_N(t)$, knowing the characteristics of the structure and the electromechanical characteristics of the shakers (Refs. 16, 17). Assuming that the desired accelerations $a_1(t)$, $a_2(t)$, $\cdots$, $a_N(t)$ are

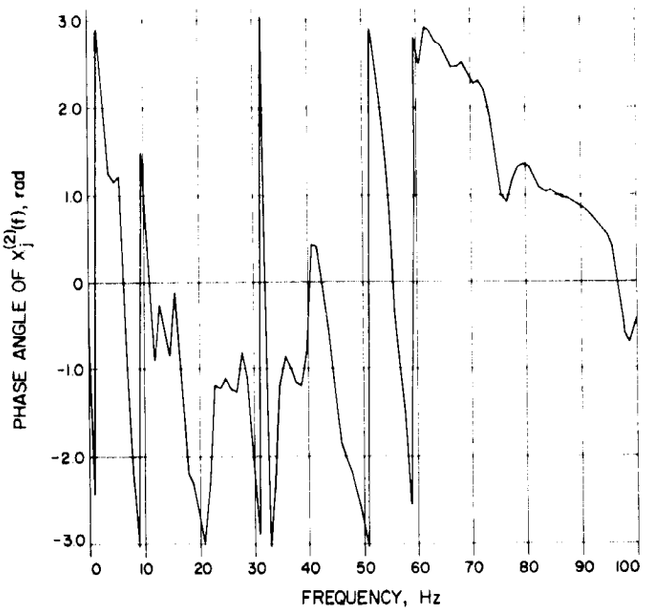

Fig. 16. Fourier transform of *Surveyor* field joint acceleration; phase angle

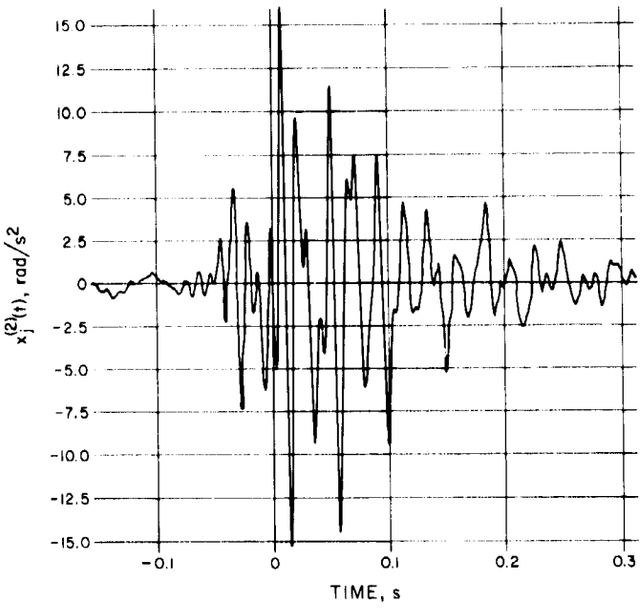

Fig. 17. Predicted *Surveyor* field joint acceleration

available as electrical signals, a shaping device, called equalizer, has to be placed in front of the power amplifiers in order to produce the proper voltages $e_1(t)$, $e_2(t)$, $\cdots$, $e_N(t)$ (Ref. 17). As an illustration, Fig. 18 represents a block diagram for an experiment run with two shakers for the excitation of a flexible beam at two points P_1 and P_2. Only the two points P_1 and P_2 are of interest for the electromechanical system formed by the shaker and the beam. The transfer functions for the two input voltages e_1 and e_2 and the responses a_1 and a_2 completely describe the electromechanical system. It is therefore more expedient to make experimental measurements of these transfer functions than to make a complete experimental model survey and use Eq. (3) to obtain the transfer functions. Once these transfer functions have been measured, the problem is to assemble an equalizer, the transfer functions of which are the inverse of those just measured. Since the system under test can be modeled as a collection of natural modes, the equalizer is constructed with operational amplifiers representing an analog simulation of single degrees of freedom. The characteristics of these degrees of freedom are determined in such a way that the simulated transfer functions fit the inverse of the measured transfer functions (Ref. 17).

V. Conclusions

Major conclusions that can be drawn as a result of these studies are that the transfer-function concept has a broad range of applications in the design, analysis and realistic testing of space vehicle systems. The technique of transfer-function coupling of subsystems is particularly useful in connection with experimental work in which only the subsystems are amenable to measurements, the experimental equipment substantially influences the measured results, and certain subsystems already have flight qualifications, e.g., boosters.

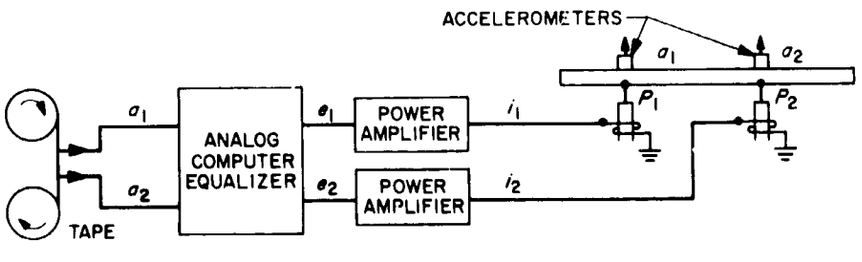

Fig. 18. Analog structure test arrangement

References

1. Heer, E., "Coupled Systems Subjected to Determinate and Random Input," *Int. J. Solids Structures*, Vol. 3, pp. 155–166, 1967.

2. Heer, E., and Lutes, L. D., "Application of the Mechanical Receptance Coupling Principle to Spacecraft Systems," paper presented at the 38th Shock and Vibration Symposium, May 1968; see also *Shock and Vibration Bulletin*, No. 38, Part II, August 1968.

3. Holzer, H., *Die Berechnung der Drehschwingungen*, Springer, Berlin, 1921.

4. Myklstad, N. O., *Vibration Analysis*, McGraw-Hill, New York, 1944.

5. Pestel, C. E., and Leckie, F. A., *Matrix Methods in Elasto Mechanics*, McGraw-Hill, New York, 1963.

6. Hurty, W. C., "Dynamic Analysis of Structural Systems Using Component Modes," *AIAA J.*, Vol. 3, p. 678, 1965.

7. Duncan, W. J., "Mechanical Admittances and Their Applications to Oscillation Problems," *H. M. S. O.* (Aeronautical Research Council), Reports and Memoranda, No. 2000, London, 1947.

8. Bishop, R. E. D., and Johnson, D. C., *The Mechanics of Vibration*, Cambridge University Press, 1960.

9. Yu, Y. Y., "Dynamics of Large Flexible Space Vehicle Systems Subjected to Arbitrary Force and Motion Inputs," paper presented at the 18th International Astronautical Congress, Belgrade, September 1967; published in the Congress Proceedings.

10. Bamford, R. M., *A Modal Combination Program for Dynamic Analysis of Structures*, Technical Memorandum 33-290, Rev. 1, Jet Propulsion Laboratory, Pasadena, Calif., July 1967.

11. Holbeck, H. J., Arthurs, T. D., and Gaugh, W. J., "Structural Dynamic Analysis of the *Mariner Mars '69* Spacecraft," *Shock and Vibration Bulletin*, No. 38, Part II, August 1968.

12. Heer, E., "Receptance Coupling Program (RECEP)," in *Supporting Research and Advanced Development*, Space Programs Summary 37-49, Vol. III, pp. 159–161, Jet Propulsion Laboratory, Pasadena, Calif., May 31, 1968.

13. Lutes, L. D., and Heer, E., *Receptance Coupling of Structural Components Near a Component Resonance Frequency*, Technical Memorandum 33-411, Jet Propulsion Laboratory, Pasadena, Calif., Oct. 15, 1968.

14. Trubert, M. R., *Use of Ranger Flight Data in the Synthesis of a Torsional Acceleration Transient for Surveyor Vibration Qualification Testing*, Technical Memorandum 33-237, Jet Propulsion Laboratory, Pasadena, Calif., April 1966.

15. Trubert, M. R., *A Fourier Transform Technique for the Prediction of Torsional Transients for a Spacecraft Using the Same Booster*, Technical Memorandum 33-350, Jet Propulsion Laboratory, Pasadena, Calif., October 1967.

References (contd)

16. Trubert, M. R., "Structural and Electromechanical Interaction in the Multiple Exciter Technique for Random Vibration Testing," *J. Acoust. Soc. Am.*, Vol. 41, No. 5, May 1967.

17. Trubert, M. R., "An Analog Technique for the Equalization of Multiple Electromagnetic Shakers for Environmental Testing," *J. Spacecraft Rockets*, Vol. 5, No. 12, December 1968, pp. 1438–43.